A case study of using cosmic ray muons to monitor supercritical CO_2 migration in geological formations[1]

Jinjin Zhong [a], Xi Jiang [b,*]

[a] Department of Safety Science Engineering & State Key Laboratory of Fire Science, University of Science and Technology of China, Hefei, Anhui 230026, China

[b] Engineering Department, Lancaster University, Lancaster LA1 4YR, United Kingdom

[*] Corresponding author. E-mail: x.jiang@lancaster.ac.uk; Tel: (+44) 1524 592439

Highlights

- Carbon storage monitoring using cosmic ray muons is investigated.
- The accuracy of the method in terms of its resolution is studied.
- The muon propagation process causes energy loss and results in attenuation.
- The muon scattering effect which may lower the spatial resolution is evaluated.
- The monitoring method may be more applicable and effective for shallow monitoring.

Abstract

In carbon dioxide (CO_2) geological storage, the monitoring of the injected CO_2 migration in underground storage is essential to understanding storage process and ensuring storage safety. An effective monitoring system will be required for decades into the future during storage phase to indicate the location where the injected fluids have extended to. A novel radiographic probing technique using naturally occurring cosmic ray muon radiations was introduced in recent years as a promising continuous and cost-effective candidate method. This method utilizes the ability of different materials to attenuate muons as the detection property. The feasibility of this technique still needs to be investigated in terms of higher simulation accuracy, the intrinsic spatial resolution, and response sensitivity for storage with impurities. In this study, simulations are performed to understand the sensitivity of this method in responding to the presence of the injected fluids in saline aquifer formations. The energy spectrum of the cosmic ray muons for different zenith angles at sea level is sampled according to the modified Gaisser's formula. The muon propagation process has been simulated with high fidelity by detailed description of different materials involved in the deployed geological model. The muon attenuation along different paths carries information on the interior of a monitored region and the muon scattering effect may lower the accuracy to locate the fluids. The intrinsic spatial resolution of this method is thus analysed and found to be at a scale of several meters. This method aims to provide the basis for understanding the injected fluids behaviour. The simulations show that the method is feasible and the injected fluids in saline aquifers can be identified with a high sensitivity.

Keywords: carbon storage; cosmic ray muon; feasibility; Monte Carlo; radiography; site monitoring.

---

1 This paper was presented at the 7th International Conference on Applied Energy (ICAE2015), March 28-31, 2015, Abu Dhabi, UAE (Original paper title: "A feasibility study of using cosmic ray muons to monitor supercritical CO_2 migration in geological formations" and Paper No.: **369**).

1. Introduction

Carbon dioxide capture and storage (CCS) may prove to be the most viable way to reduce CO_2 emission into the atmosphere on an industrial scale [1, 2]. Instead of allowing carbon dioxide to be directly emitted into the atmosphere, CCS technologies would capture a large amount of CO_2 from carbon-based power plants, compress it into supercritical state, transport and finally inject it into well-characterized underground porous formations, which usually lie at depths of more than 800 meters below the ground surface [3]. Since purification of the fossil fuel-derived CO_2 would account for a large proportion of the total costs, CO_2 feed-in will often contain impurities, which could be N_2, O_2, H_2S, and/or SO_x [4-6]. CCS projects are aimed at sealing the injected fluids in geological formations effectively. However, there is no guarantee that the goal of carbon sequestration can be fulfilled without complexities and the injected fluids will stay underground safely forever. Once injected, the fluids would migrate both upward and laterally under the driving forces of buoyancy and the pressure difference between the injection zone and the ambient zones. Site monitoring is required for decades into the future in view of the expected time scales for permanent storage [7]. Monitoring systems can be classified into two categories, i.e. shallow and deep monitoring [8]. Deep monitoring of the injected fluids is to identify the location where they have extended to for reasons of process control, storage safety and effectiveness, and verification and modification of the numerical prediction models. When the fluids appear in unintended regions like areas near depleted wells, natural geological faults, and fractures in upper cap rocks, it may pose a threat of leakage. Deep monitoring can help reduce the occurring rate of leakage by site-specific risk assessment together with relative remediation measures, provide a basis for improving the prediction models and also help better understand the fluids migration behaviour in deep storage [9, 10]. When leakage takes place, shallow monitoring is needed to locate it. Existing monitoring techniques tested in experiments and ongoing pilot projects include geophysical and geochemical measurements [11-16]. These methods tend to be episodic, and the frequency and extent of monitoring are important problems to be settled in a practical storage phase. In view of this, a continuous monitoring method is also needed to provide a continuous measurement for observing dynamic reservoir behaviour.

A new method, cosmic ray muon radiography, was introduced in recent years to effectively address this need in a way with no destruction to the storage integrity [17]. If the dynamically extending saturated region by the injected fluids can be determined using this method, measurements for more information can be regulated accordingly. This work is focused on the feasibility of the method in respect of the spatial resolution and sensitivity for responding to storage scenarios involving impurities. Based on the principle of traditional radiography (represented by X-ray scanning of a human body), cosmic ray muon radiography uses the ability of different materials to attenuate the cosmic ray muons as the detection property of a targeted object, and measures the statistical penetrating muon events along different paths through a monitored object as the information source for probing the interior of the objet. In radiography, energy of the used ray particles should be chosen so that the mean range of the particles is comparable to the thickness of the tested object. The larger or denser a targeted object is, the higher the energy of the used particles has to be. Eventually the onset of pair production ($2\gamma \rightarrow e^- + e^+$) with the increase of the required photon energy sets a limit to the size of the samples that can be imaged by this method [18]. However, cosmic ray muons possess some unique characteristics and can be used for detecting the interior of geophysical-scale objects, in a way similar to applications in other areas found by X-rays and γ-rays.

Cosmic ray muons are naturally occurring and highly penetrating particles continuously arriving at the earth surface from different zenith angles. At sea level, the energy spectrum of cosmic ray muons has a wide range from extremely low value to hundreds of TeV, which is almost time-independent [19], making cosmic ray muons a suitable radiation source for radiography. The small variations related to several factors in the energy spectrum has been well studied, and the ultimate effects on imaging can be adjusted by placing a muon detector above the monitored area in practical applications [20]. Besides, by virtue of the weak interactions with matter, muons with an initial energy of tens of GeV can reach depths of tens of meters in standard rock, far beyond the penetration limit of X-rays or γ-rays under the same conditions. In fact, cosmic ray muon radiography has been successfully applied for geophysical studies [19, 21], such as search for hidden chambers in the Kephren Pyramid [22], measurements of the thickness of snow layers on a mountain and investigation of volcano structures [23]. It has been confirmed that this technology is capable of mapping volcano structures with higher resolutions than other geophysical technologies [24]. The idea of this method can also be easily extended to measurements of time-dependent changes occurring within a target [25]. With a baseline measurement, the following measurements could provide the interior variation by comparing the statistical information of the penetrating events along different directions. By virtue of this, the spot where change has happened can be determined and located in two dimensions. In order to identify the three-dimensional site, two or more detection systems will be required [26].

Previous work [17] on the feasibility study of cosmic ray muon radiography was based on the storage scenario of carbon sequestration in saline aquifer. The preliminary simplified simulation results showed that this technique can respond to the presence of supercritical CO_2 in deep reservoirs with a relatively high sensitivity. In this previous study, mean density was the only varying quantity considered before and after the saturation of the injected fluid in the monitored region, while the influence of other important factors such as change in material composition on measurements was neglected. To fully study the feasibility of this method, more investigations are needed to better understand its responding sensitivity to the injected fluids and other parameters such as the intrinsic spatial resolution that can be achieved. With these purposes, two aspects of this method have been investigated in this study. Firstly, the scattering effect of muons during propagation in matter was evaluated, which would determine the intrinsic spatial resolution. Secondly, the sensitivity of the statistical penetrating muon events to the injected fluids in saline aquifer formations was investigated. Two different storage scenarios, storage of pure CO_2 and with impurities H_2S and N_2 involved, were investigated respectively. Given a muon detector with a certain area and an angular acceptance region, the area that is within the scanning scope of this detector is determined. The muon detector receives the penetrating cosmic muons through the volume above and adjacent to it. The sensitivity of the method is analysed and determined by comparing the statistical information on the penetrating muon events for saturation cases of different fluid concentrations with those for the baseline case prior to injection of the fluids.

2. Cosmic ray muon radiography

The process of the application of cosmic ray muon radiography in detecting time-dependent change within an object is outlined here. In this technology, a muon detector is placed in an underground detecting room, aiming to monitor an object that is above and adjacent to it. The incident cosmic ray muons hit the ground surface, and then propagate through the object. The ones with sufficient energy to penetrate the object are recorded by the muon detector. The muon detector can record the penetrating cosmic muons from different directions with a certain intrinsic angular resolution which is determined by the detector structure. The penetration behaviour of the muon flux carries information on the material property along the muon path lines of the measurement period. Time-dependent changes within the object may be inferred by continuous measurements and analysis. If variations of matter in material composition and density happened within the scanning scope of the detector, the counting of muon events at corresponding arriving angles would change accordingly.

However, during the propagation process muons also experience stochastic scattering all along the way except for losing energy. The accumulation of the scattering effect may lead to a certain deflection from their original directions [27]. Considering that the penetrating muons recorded from a specific direction (θ, Φ), with θ and Φ representing the zenith and azimuth angles of muons respectively, may have been actually deflected to a certain degree, the scattering effect could have a negative impact on locating the region where changes actually take place. In general, the accumulated deflection angles determine the intrinsic spatial resolution of this method which should be evaluated in deep monitoring applications in CCS. The spatial resolution should be at a reasonable scale to achieve good performance in detecting.

The measurements performed at one detection spot can only identify changes either in the mean density or in the material composition along the muon paths, so they cannot provide information on the specific site where changes take place. Nevertheless, changes in lateral direction within the monitored domain could be effectively measured in this way. In order to locate the specific area, measurements performed at more than two spots at the same time are needed to construct a three-dimensional monitoring system. The three-dimensional positioning is beyond the scope of this work, which is mainly focused on the problem of the sensitivity of this technology in CCS site monitoring.

2.1 Cosmic ray muon source

The earth is continuously bombarded by primary rays from outer space. At an altitude of about 32 km, primary rays interact with the atmosphere, producing large amounts of secondary particles, which travel down through the atmosphere to the earth surface. When arriving at sea level, most of them are muons, accounting for about 63% of the energy [28], with an approximately time-independent energy spectrum ranging widely from GeV to PeV. In a simulation study, an accurate knowledge of the incident cosmic ray muon flux is of vital importance since it is used to determine the attenuation produced by a targeted object.

Precise knowledge of the muon energy spectrum is based on numerous experimental measurements. The energy spectrum of cosmic ray muons at sea level depends on zenith angles, and is azimuthally isotropic. In this study, the muon energy spectrum for different zenith angles was taken from the modified Gaisser spectrum [29] with the best fit values for normalization and spectral index obtained by experimental measurements. The total differential flux of cosmic ray muons falls very rapidly with energy losses. As for the incident zenith angle, the cosmic muon flux in low-energy region decreases as it increases, but in high-energy region, it is the other way around. The total integrated intensity of incident cosmic ray muons at sea level is quite low, with about 1 muon per minute·cm^2. Given this situation, the exposure time may be needed to be quite long or the detection area to be fairly large to get adequate number of muons to be used as the radiation source in one measurement period. This may become a limiting factor for the applicability of this technology taking into consideration of practical conditions and requirements, such as the time needed for a specific application and the availability of space to accommodate the whole detection apparatus underground.

2.2 Muon propagation in matter

The muon is a particle having similar charge properties as the electron. They are equally charged with a spin of 1/2, except that the muon has a larger mass (207 times heavier than the electron). High-energy muons passing through matter lose energy by ionization and radiative processes - bremsstrahlung, direct production of e^-/e^+ pairs, and photonuclear interactions [29]. The mean ionization loss rate of a muon of energy E is given by the well-known Bethe-Bloch formula:

$$-\left\langle \frac{dE}{dx} \right\rangle_i = 4\pi N_A r_e^2 m_e c^2 z^2 \frac{Z}{A} \frac{1}{\beta^2} \left(\frac{1}{2} \ln \frac{2 m_e c^2 \beta^2 \gamma^2 T_{\max}}{I^2} - \beta^2 - \frac{\delta}{2} \right), \tag{1}$$

where dE/dx is expressed in MeV g^{-1} cm^2.The meanings of all the other parameters are: x stands for density length (density × length), often referred to as opacity, representing the amount of matter encountered along the path; z is the electric charge of the incident particle, scaled by $|e|$, and here for the muon, z equals to 1; A and Z are the mass number and the atomic number of the traversed material, and the unit of A is g/mole; m_e is the rest mass of the electron; r_e is the classical electron radius; $N_A = 6.023\times10^{23}$ is Avogadro's number; I is the average excitation energy depending on the property of the traversed matter, which can be approximately described as $I = 16Z^{0.9}$ eV ($Z > 1$), and it is also related to the state of molecule; δ is the density correction [30].

The energy losses caused by radiative processes are more complicated, and the evaluation can be highly accurate by virtue of improved experimental measurements. For each type of radiative interactions, the transferred energy from a muon of energy E is stochastic and can be expressed in the cross section, that is, the probability density distribution of the value of the transferred energy. The cross section for each radiative interaction can be looked up [31]. Such energy loss mechanism was illustrated by bremsstrahlung here. The cross section for bremsstrahlung is expressed in the following formula:

$$\frac{d\sigma}{dv} = \alpha^3 \left(2Z\lambda_e \frac{m_e}{m_\mu} \right)^2 \frac{1}{v} \left(\frac{4}{3} - \frac{4}{3} v + v^2 \right) \phi(\delta), \tag{2}$$

Where v is the fraction of energy transferred from the muon, α (= 1/137.036) is the fine structure constant, λ_e and m_μ are the Compton wavelength of the electron and the rest mass of the muon respectively, and $\Phi(\delta)$ is evaluated as follows

$$\phi(\delta) = \ln \frac{\frac{189 m_\mu}{m_e} Z^{-1/3}}{1 + \frac{189\sqrt{e}}{m_e} \delta Z^{-1/3}} \quad Z \le 10, \quad \phi(\delta) = \ln \frac{\frac{2}{3}\frac{189 m_\mu}{m_e} Z^{-2/3}}{1 + \frac{189\sqrt{e}}{m_e} \delta Z^{-1/3}} \quad Z > 10, \tag{3}$$

where $\delta = m_\mu^2 v / 2E(1 - v)$ is the minimum momentum transfer to the nucleus and e = 2.718. From the integral of the cross section (3) between $v_{\min}$ = 0 and $v_{\max}$ = $1\text{-}3/4\sqrt{e}(m_\mu/E)Z^{1/3}$, the mean energy loss rate caused by bremsstrahlung can be calculated as

$$-\left\langle \frac{dE}{dx} \right\rangle_b = E \frac{N}{A} \int_{v_{\min}}^{v_{\max}} v \frac{d\sigma}{dv} dv . \tag{4}$$

Following the above, the total mean energy loss rate (also referred to as the stopping power) of the muon for a single element is derived by summing up the individual contributions and can be parameterized as：

$$\begin{aligned} -\left\langle \frac{dE}{dx} \right\rangle &= -\left\langle \frac{dE}{dx} \right\rangle_i -\left\langle \frac{dE}{dx} \right\rangle_b -\left\langle \frac{dE}{dx} \right\rangle_p -\left\langle \frac{dE}{dx} \right\rangle_n \\ &= \mathrm{a}(Z, A, E) + b(Z, A, E) \cdot E , \end{aligned} \tag{5}$$

where p denotes pair production, n stands for nuclear interactions, a (Z, A, E) represents the mean ionization energy loss rate in Eq. (1) and b (Z, A, E) is the joint energy-scaled contributions of the three radiative interactions. Both a and b are functions of material type (Z and A) and slowly varying functions of E. The formula given in Eq. (5) is the mean energy loss rate of the muon in an object made of a pure element. For a compound or a mixture, the mean energy loss rate is the weighted sum of that for all the elements involved and the weight fraction for each element is computed by:

$$w_j = n_j A_j \Big/ \sum_k n_k A_k \ . \tag{6}$$

In Eq. (6), w_j stands for the mass weight of j element in a compound or mixture while n_j represents the number of j element in a compound or mixture. It follows that

$$\left\langle \frac{dE}{dx} \right\rangle = \sum_j w_j \left. \frac{dE}{dx} \right|_j . \tag{7}$$

Fig. 1 (left) shows the mean energy loss rate of muons in standard rock, brine, and CO_2. In this study, the standard rock considered is underground rock with Z/A=11/22, density=2.65 g/cm^3, while the supercritical CO_2 is considered to have density=0.75g/cm^3. In Fig. 1, the dotted symbols represent the experimental data obtained from the Particle Data Group (http://pdg.lbl.gov). From the fitted curves it can be seen that the energy loss rates for the three materials vary little from each other in the lower energy region. In the higher region, the energy loss rate is the largest for standard rock, and the least for CO_2. By taking into consideration the density of the materials, the mean physical range of muons of different energy in CO_2 gas, supercritical CO_2 and water is calculated and demonstrated in Fig. 1 (right). It can be seen that muons with a certain incident energy can penetrate the furthest distance in supercritical CO_2, and that the penetration ability in CO_2 gas is higher than in water. In view of this, it can be deduced that for an object made up of the mixture of standard rock, water and CO_2 (either in supercritical state or gaseous state), the penetrating cosmic ray muon flux would increase with more displacement of water by CO_2 (either in gaseous or supercritical state).

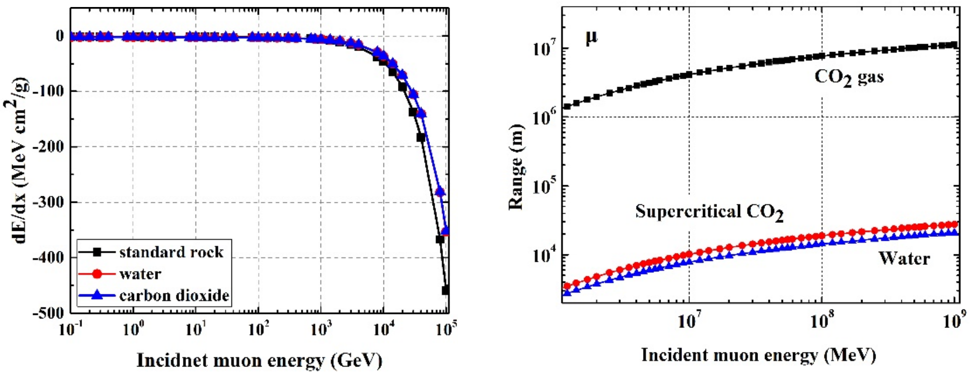

Fig. 1. Left: The mean energy loss rate or stopping power of muons in standard rock, brine and CO_2 with experimental data from the Particle Data Group (http://pdg.lbl.gov); Right: The muon range (m) in gaseous CO_2, supercritical CO_2 and water with different initial energy.

Apart from losing energy during propagation in a medium, muons are also continuously scattered by the Coulomb force of both atomic nuclei and electrons along their paths. The momentum of muons will slightly affected each time when scattering takes place, and multiple scattering processes lead to muon deflections from their original direction to a certain extent. The angular distribution of muons becomes broader and the lateral deflection grows larger as muons propagate through matter. Thus, multiple scattering effects may have an impact on the spatial resolution of this technology, since the direction of the penetrating muons accepted by the corresponding image pixel of the muon detector may have been deflected from the original direction with an angle larger than the angular resolution of this pixel.

Precise knowledge of the muon propagation process in matter makes it possible to theoretically calculate the minimum energy E_{min} for cosmic ray muons to penetrate a given object from a certain incident point (x_0, y_0, z_0) and direction (zenith angle of θ_0, azimuthal angle of Φ_0). By integration of the energy spectrum of the incident cosmic ray muons with $E_{\rm min}$ as the lower energy limit, the intensity I (θ_0, Φ_0) of the penetrating cosmic ray muons in an exposure duration ΔT can be obtained corresponding to the interior state of the object along the muon path. When changes either in the mean density or the material composition happen to the object, the value of E_{min} and the resulting integrated intensity I (θ_0, Φ_0) varies. It is necessary to emphasize that E_{min} can only be defined as a quantity of statistical average, because of the stochastic fluctuations of the muon energy losses from the radiative processes and the muon multiple scattering effect, which cause the stopping power fluctuations and range straggling of muons respectively under the same conditions of the object. Therefore, in practical measurements, the deviation between two separate measurements needs to be large enough to certify that the variation in measured I (θ_0, Φ_0) originates from the change in the object rather than the intrinsic fluctuations, and the identification should be interpreted in terms of confidence level statistically.

Because of the multiplicity of the energy loss mechanisms, it is difficult to precisely derive the range of the muon in a medium in an analytical form given in terms of the initial energy E_0. Besides, fluctuations of the transferred energy from muons in the stochastic radiative processes would lead to stopping power fluctuations and range straggling in practice. A detailed treatment of muons propagation resorts to high-fidelity simulations. For the stochastic processes with well-known cross sections, Monte Carlo modelling provides an effective approach to simulate the specific processes with a high accuracy, which can sample each kind of interaction (including multiple scattering effects) according to their cross sections for each step along the muon path in matter.

In practical measurements the recorded muons in two separate measurement periods may vary with no actual change happening to the inside of the targeted object, due to the fact that the intrinsic fluctuations of this technology originating from the stochastic processes along the muon path also play a role in the variation of detected muon events. The stochastic processes have been investigated and it is known that the counts of penetrating muons through a targeted object follow the statistical law under the same condition of the targeted object. Analysis on the phenomenon can only be made on the basis of adequate penetrating muon events. When the recorded number N of muon events penetrating the targeted object in one detection period is large enough ($N >> 16$), N can be seen as the mean number statistically, and the counts for the following measurements with no actual change taking place can be described by the Gaussian distribution with the standard deviation $\sigma = N^{1/2}$ [32]. Assuming that the difference between the counts in another measurement period and N is equal to Δ_0, when Δ_0 is equal to σ, there is a probability of 31.73% for the difference to be originated from the intrinsic fluctuation or systematic error. From another point of view, change within the monitored object can be resolved or identified with a confidence level of 68.27%. Confidence level for identification of change in the targeted object is generally represented by k times of standard deviation. With Δ_0 or the value of k increases, the increase of the probability for the variation due to changes within the object becomes larger as specifically shown in Table 1 by (1 - F (Δ_0)). In practical measurements, k is usually required to be larger than 1 to indicate internal change of the object rather than the intrinsic fluctuations of this method. The value of k has to be larger if high accuracy is needed.

Table 1. Confidence level for the variation (Δ_0) of the penetrating muon events between two separate measurements originated from the change within a monitored object.

Δ_0/σ	0	0.6745	1	1.6449	2	3
F(Δ_0)	1.0000	0.5000	0.3173	0.1000	0.0455	0.0027
1-F(Δ_0)	0	0.5000	0.6827	0.9000	0.9545	0.9973

3. Monitored site model

In this study, the storage scenario of carbon sequestration in deep saline aquifers is investigated to examine the performance of cosmic ray muon radiography in site monitoring by Monte Carlo simulations. Deep saline aquifers with overlying impermeable formations are the most widely adopted options for the geological storage of pure CO_2 or impure CO_2 streams with other contaminant gases involved. In the process of injection and storage, the injected fluids displace some of the salty water and migrate to the regions with lower pressure before they are immobilized and permanently sealed in the storage. Cosmic ray muon radiography performed in a specific site to be monitored was examined to identify the change caused by the saturation of the injected fluids in the formations.

The first model was deployed for deep monitoring and is briefly described as follows. The monitored area in the simplified application scenario comprised of two layers and the surface of the area is assumed to be flat and at sea level. The upper layer is cap rock comprised of standard rock, and the lower layer is a saline aquifer layer which is made up of standard rock with a porosity of 35% initially saturated with brine. The brine is assumed to be composed of NaCl and H_2O, and the density is 1.1 g/cm^3. The cap rock is 1000 m thick, while the saline aquifer is 250 m thick underneath the cap rock. The material properties involved in the monitored site model are shown in Table 2. As supercritical CO_2 migrates in the saline aquifer, the mean density and material composition in the saline aquifer change with its presence associated with the migration of CO_2 into or out of the targeted area. The sensitivity of cosmic ray muon radiography to monitor and identify such changes, i.e., the sensitivity of penetrating cosmic ray muon flux in one measurement period to such changes, was investigated by changing CO_2 volume fraction in the monitored site model from 0% to 15% in the different cases studied. For each case, the distribution of the mixture of standard rock, brine and supercritical CO_2 is set to be homogeneous in the saline aquifer, and the monitored area is deemed to be constant within one measurement period.

Table 2. The properties of the materials involved in the model.

Formation properties	Standard rock	Supercritical CO_2	Brine	
			NaCl	H_2O
Atomic number	11	7.33	14.00	3.33
Atomic mass (g/mole)	22	14.67	29.23	6.00
Density (g/cm^3)	2.65	0.67	2.1075-2.02 (changing with CO_2 volume fraction variance)	

The second model for shallow monitoring considered a multi-layered storage formation from the literature [33]. It is a sequence of 60 m thick aquifers and 100 m thick aquitards extending from the deep saline storage formation to the uppermost freshwater aquifer. Each layer is assumed to be made up of standard rock and pores filled with brine or freshwater. The material property is obtained from the NIST chemistry book (http://webbook.nist.gov/chemistry/fluid/). The porosity is 0.05 in the aquitards and 0.2 in the aquifers respectively, and the hydrogeologic properties are homogeneous in the same layers in the simulation processes. This study investigates the sensitivity of using this method to monitor leakage of the injected fluids into the second aquifer from the top. The leakage scenarios include pure CO_2 gas and impure CO_2 with N_2, H_2S and SO_2.

4. Simulation results

The propagation process of cosmic ray muons crossing the monitored site model was simulated by Geant4, a Monte-Carlo toolkit for simulation of particle propagation in matter with high fidelity [34, 35]. Geant4 was developed as an object-oriented toolkit and has gained wide applications in high energy physics as well as studies in medical and space sciences. It allows users to produce a radiation source of their own needs. In this simulation study, the cosmic ray muons are produced by Monte-Carlo sampling according to an energy-spectrum histogram generated from the modified Gaisser formula. The width of each of the histogram bin is 1 GeV and the energy was sampled linearly within each histogram bin, which means the sampling of the cosmic ray muons is highly accurate. The setup of the geometry and the material composition of the target can be well described and precisely implemented. In the simulation process, a cosmic ray muon is sampled at the beginning of a simulated event and then radiates through the target. The passage of the muon through matter is accomplished by Monte-Carlo modelling. For each step along the muon path in matter, each kind of stochastic interaction between the muon and matter, including the muon multiple scattering effect, is sampled according to their respective cross sections by Monte-Carlo modelling. The availability of the latest updated cross sections of the muon in different kinds of elements allows accurate modelling of the muon propagation process in matter.

Because the muon behaviour in matter is stochastic, the outgoing energy of a muon with a given incident energy and direction is uncertain and forms a spectrum. The possibility of using the outgoing energy spectrum variation as an accompanying information source of the inner change in the targeted object is investigated. Fig. 2 shows that the CO_2 volume fraction variations have little influence on the normalized energy spectrum shapes, which is shown by the probability density distribution of the penetrating muon energy. The results indicate that it would not work by considering the outgoing energy spectrum to interpret the inner change caused by the variation in CO_2 displacement of the in situ brine within the monitored volume.

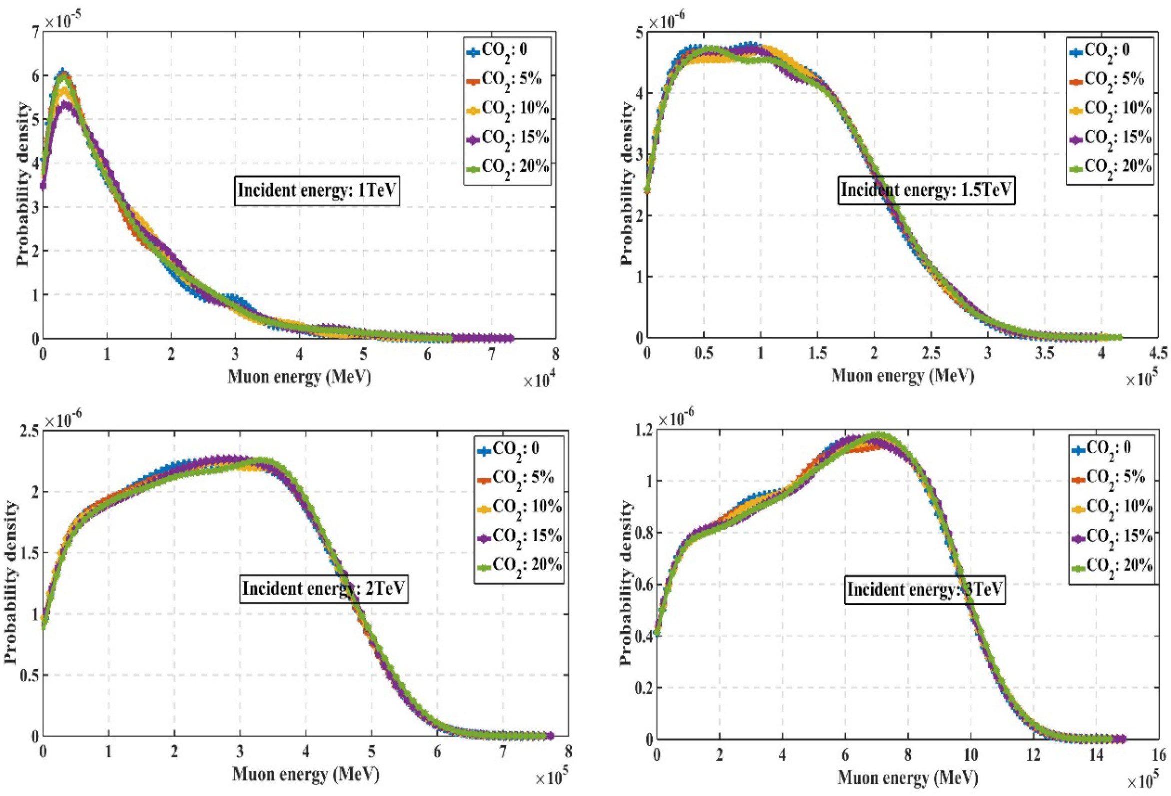

Fig. 2. The outgoing energy spectrum of the muons vertically penetrating the entire storage area (the first storage model) with certain incident energy.

The muon scattering effect and accumulated deflections when arriving at the detection panel were studied for deep monitoring. The largest angle of muon deflection when arriving at plane determines the intrinsic spatial resolution in a specific application. Fig. 3 demonstrates the spatial resolution that can be achieved by the cosmic muons from zenith angle 0° and 10°. The results indicate that this method can achieve a spatial resolution ranging from 10 m to 20 m in deep monitoring application. Compared with the target at a scale of hundreds of meters, the spatial resolution is at a relatively high level.

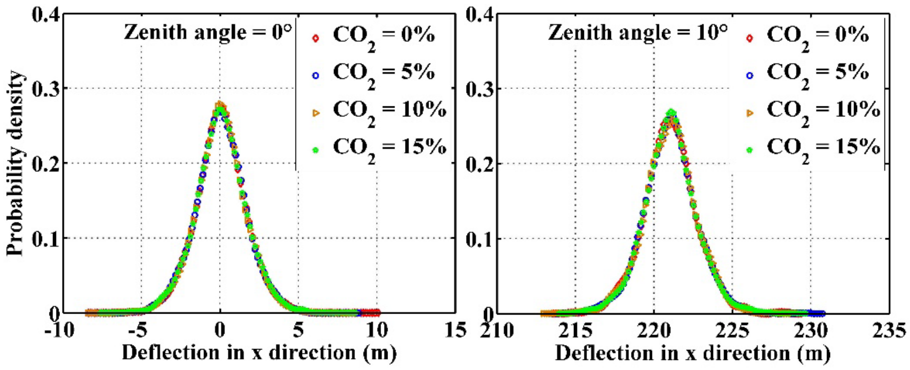

Fig. 3. The deflections of the cosmic ray muons incident from zenith angle 0° and 10° when arriving at the detector placed adjacent and beneath the storage.

In the sensitivity study for deep monitoring, the incident cosmic ray muons are sampled according to the modified Gaisser formula. By increasing the amount of supercritical CO_2 in the saline aquifer, the sensitivity of the penetrating cosmic ray muon intensity to the change within the monitored site was investigated. The case study of the monitored site model with no supercritical CO_2 in the saline aquifer corresponds to the baseline measurement in practice. The simulation results in Fig. 4 and Fig. 5 show with the increase of the supercritical CO_2 composition in the saline aquifer, the penetrating number of cosmic ray muons fluctuates locally but increases globally. The fluctuations are due to the intrinsic statistical attribute of this method and meanwhile, the penetrating muon events are not large enough to reach a level that can be statistically averaged. A sample of vertically incident cosmic muon events (corresponding to one measurement period of one year and a detection area of about 25 m^2) was first used in the simulation, and the muon detector was set to receive the penetrating muons whose directions fall into a zenith angle range from 0 to 10 mrad. The result in Fig. 4 shows that the detectable amount of supercritical CO_2 using vertically incident cosmic muons is about 5% measured in volume fraction in deep saline aquifers. A second set of simulations were made with a shorter measurement period of 100 days, and the results in Fig. 5 show that the sensitivity decreases with less sampled cosmic muons, as can be easily deduced from the statistics. About 8% supercritical CO_2 measured in volume fraction can be identified by the cosmic muons from zenith angle 0°, and about 11% can be detected by cosmic muons from zenith angle 10°.

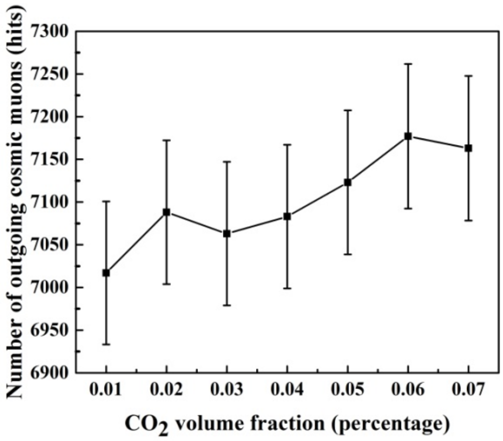

Fig. 4. The variation in the outgoing number of the vertically incident cosmic muons under different volume fractions of supercritical CO_2 in the saline aquifer of the underground storage with measurement period of 1 year.

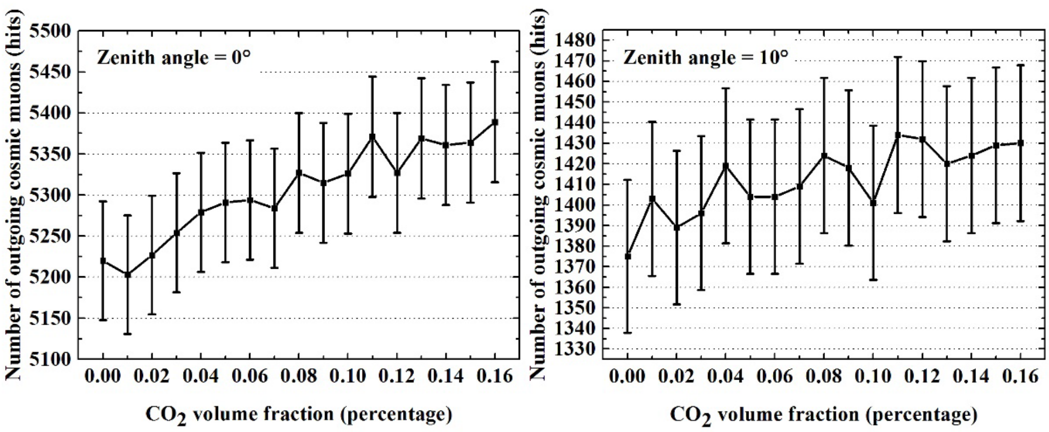

Fig. 5. The variation in the penetrating cosmic muons number (from zenith angle 0° and 10° respectively) under different volume fractions of supercritical CO_2 with measurement period of 100 days.

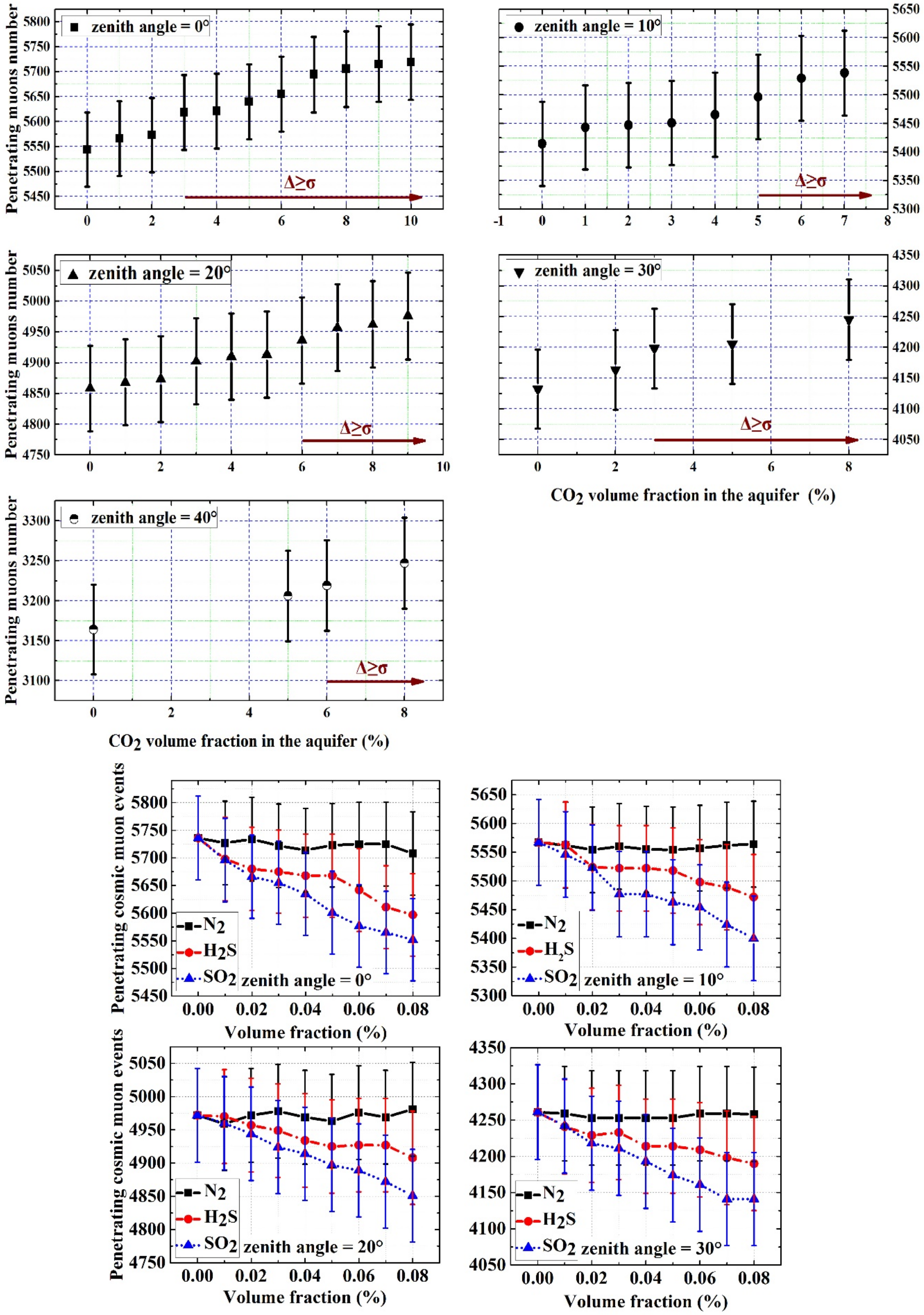

Fig. 6. Upper: The penetrating number of cosmic muons recorded for the baseline case and different cases of CO_2 leakage in the shallowest aquifer using a muon detector with a surface area of 1×1 m^2 and a measurement period of 3 days. Lower: the penetrating cosmic muons from zenith angle 0°, 10°, 20°, 30° under various leakage scenarios with different

impurities involved.

Fig. 6 demonstrates the results of the sensitivity study for shallow monitoring. It can be seen that the monitoring effectiveness improves dramatically compared with deep monitoring. The sensitivity for detecting the presence of CO_2 is much higher with a reduced measurement period and a smaller detection area. Leakage with impurities involved was considered and their impact on the sensitivity is evaluated. As deduced from the lower set of the sub-figures, N_2-mixed impurities has a negligible influence on the detection sensitivity, while SO_2-mixed impurities has the most prominent influence on the detection sensitivity and can lower the sensitivity by 10% of CO_2 volume fraction. H_2S-mixed impurities could lower the detection sensitivity by about 6% of CO_2 volume fraction. The results on the effects of impurity are of practical relevance to geological carbon storage. In fact, the concentration of the impurities in practical situations is rather low. This method can apply to the SO_2-mixed situations with a lower sensitivity. Overall the method performs much better in shallow monitoring than in deep detection because the intensity of cosmic ray muon events becomes higher with decreasing depths. And the statistical requirement can be more easily met at shallower depths.

The feasibility of radiographic method depends on two aspects, the sensitivity of the method and the spatial resolution. The simulations conducted for the applications of deep and shallow monitoring have showed the feasibility of this technique in CCS monitoring. Because the detection is based on statistical information of the cosmic ray muon events to be used, the sensitivity would be higher with the increase of the events number as can be seen from Fig. 6. The total number is determined by the measurement period and the detection area. In a specific application, trade-off should be made between the detection area and the detection period according to practical requirements, including consideration of the characteristic time for the dynamic behaviour of geological carbon storage in CCS and the specific geological conditions for the detection system to be placed.

5. Concluding remarks

Monitoring of carbon storage can help understand the dynamic behaviour of storage reservoirs. The knowledge of the supercritical CO_2 migration can provide a basis for mitigation measures as well as modification and verification of numerical prediction models. Timely detection and location of the leakage region permeated by the injected fluids is of vital importance for remediation measures to be taken effectively. This paper presented a feasibility study of cosmic ray muon radiography as a promising continuous and cost-effective monitoring method. Based on the principle of traditional radiographic imaging, the feasibility of this technology was investigated mainly from two aspects using a simplified application scenario of carbon sequestration in deep saline aquifer formations. The first aspect examined is about the intrinsic spatial resolution that is determined by the muon scattering effect, and the second aspect is the sensitivity of this method to the presence of CO_2, either in the form of supercritical state in deep storage or in the gaseous state in shallow formations in the case of leakage taking place. Furthermore, in the application for detecting shallow leakage, the influence of impurities on the detection sensitivity is evaluated. Besides, the muon outgoing energy spectrum is also investigated with regard to the possibility of using it as a possible probing parameter, but it turns out that it is not sensible to the CO_2 displacement of the in situ pore formation.

The spatial resolution is an important index for a radiographic probing technology in which the stopping power of the muon in matter is the imaging parameter. For this technology, the spatial resolution was determined by the muon scattering effect and found to be at a relatively high level of a scale of ten meters. In deep monitoring application, the presence of supercritical CO_2 can be identified in the region within its scanning scope at a relatively high level of about 5%. Since the probing method is based on statistical analyses of adequate number of cosmic muon event, the higher the sensitivity is, the more the required cosmic muon events are. Since the number of events is determined by the measurement period and the detection area, the measurement period should be decided to meet the practical requirements associated with the characteristic time for the underground behaviour. For the same reason, this method performs better in shallow monitoring application considering that the cosmic ray muon intensity is higher at shallower depths. For a period of several days and a detection area of several m^2, the detectable CO_2 leakage can be as low as about 5%. This method also applies to the leakage situations with N_2 involved regardless of the concentration and H_2S- and SO_2-mixed leakage situations when the impurity concentration is not too high. A significant advantage of this technique is that it can provide continuous measurements. In deep monitoring, it could help determine the frequency and occasion for other measurements to be taken, and in shallow monitoring, it could identify the fluid leakage timely. The specific region, either the newly extended area in deep storage formations or the leakage area saturated with intruding fluids in shallow formations, can also be located by constructing a three-dimensional detection system from two or more detection spots. Cosmic muons from various directions can be utilized, and this study has investigated the feasibility of this newly introduced method in CCS monitoring on a wide range. Because cosmic ray muons are naturally and continuously occurring and the muon detectors that can be applied are available at relatively low costs, this method could serve as an effective means to perform continuous site monitoring for carbon storage, complementary to other monitoring techniques.

References

[1] Metz B, Davidson O, De Coninck H, Loos M, and Meyer L. Carbon dioxide capture and storage. 2005.

[2] Torp TA and Gale J. Demonstrating storage of CO_2 in geological reservoirs: the Sleipner and SACS projects. *Energy* 2004;**29**:1361-1369.

[3] Benson SM and Cole DR. CO_2 sequestration in deep sedimentary formations. *Elements* 2008;**4**:325-331.

[4] Last GV and Schmick MT, *Identification and selection of major carbon dioxide stream compositions*: Pacific Northwest National Laboratory, 2011.

[5] Liu H and Shao Y. Predictions of the impurities in the CO_2 stream of an oxy-coal combustion plant. *Applied Energy* 2010;**87**:3162-3170.

[6] Li H, Yan J, and Anheden M. Impurity impacts on the purification process in oxy-fuel combustion based CO_2 capture and storage system. *Applied Energy* 2009;**86**:202-213.

[7] Haszeldine RS. Carbon capture and storage: how green can black be? *Science* 2009;**325**:1647-1652.

[8] Hannis SD. Monitoring the geological storage of CO_2. 201368-96.

[9] Jiang X, Hassan WA, and Gluyas J. Modelling and monitoring of geological carbon storage: A perspective on cross-validation. *Applied Energy* 2013;**112**:784-792.

[10] Emberley S, Hutcheon I, Shevalier M, Durocher K, Mayer B, Gunter W, *et al.* Monitoring of fluid–rock interaction and CO_2 storage through produced fluid sampling at the Weyburn CO_2-injection enhanced oil recovery site, Saskatchewan, Canada. *Applied Geochemistry* 2005;**20**:1131-1157.

[11] Dai K, Li X, Song X, Chen G, Pan Y, and Huang Z. Monitoring of CO_2 geological storage based on the passive surface waves. *International Journal of Mining Science and Technology* 2014;**24**:707-711.

[12] Padhi A, Mallick S, Behzadi H, and Alvarado V. Efficient modeling of seismic signature of patchy saturation for time lapse monitoring of carbon sequestrated deep saline reservoirs. *Applied Energy* 2014;**114**:445-455.

[13] Emberley S, Hutcheon I, Shevalier M, Durocher K, Gunter W, and Perkins E. Geochemical monitoring of fluid-rock interaction and CO_2 storage at the Weyburn CO_2-injection enhanced oil recovery site, Saskatchewan, Canada. *Energy* 2004;**29**:1393-1401.

[14] Arts R, Eiken O, Chadwick A, Zweigel P, Van Der Meer L, and Zinszner B. Monitoring of CO_2 injected at Sleipner using time-lapse seismic data. *Energy* 2004;**29**:1383-1392.

[15] Park Y-C, Huh D-G, and Park C-H. A Sensitivity Study of Pressure Monitoring to Detect Fluid Leakage from Geological CO2 Storage Site. *Energy Procedia* 2013;**37**:4207-4214.

[16] Wei N, Li X, Wang Y, Zhu Q, Liu S, Liu N, *et al.* Geochemical impact of aquifer storage for impure CO_2 containing O_2 and N_2: Tongliao field experiment. *Applied Energy* 2015;**145**:198-210.

[17] Kudryavtsev VA, Spooner NJC, Gluyas J, Fung C, and Coleman M. Monitoring subsurface CO_2 emplacement and security of storage using muon tomography. *International Journal of Greenhouse Gas Control* 2012;**11**:21-24.

[18] Baek C-H, An SJ, Kim H-I, Kwak S-W, and Chung YH. Development of a pinhole gamma camera for environmental monitoring. *Radiation Measurements* 2013;**59**:114-118.

[19] Lesparre N, Gibert D, Marteau J, Déclais Y, Carbone D, and Galichet E. Geophysical muon imaging: feasibility and limits. *Geophysical Journal International* 2010;**183**:1348-1361.

[20] Borozdin KN, Hogan GE, Morris C, Priedhorsky WC, Saunders A, Schultz LJ, *et al.* Surveillance: Radiographic imaging with cosmic-ray muons. *Nature* 2003;**422**:277-277.

[21] Marteau J, Gibert D, Lesparre N, Nicollin F, Noli P, and Giacoppo F. Muons tomography applied to geosciences and volcanology. *Nuclear Instruments and Methods in Physics Research Section A: Accelerators, Spectrometers, Detectors and Associated Equipment* 2012;**695**:23-28.

[22] Burkhard J, Fakhry A, Girgis A, Goneid A, Moussa AH, and Mohammed-Sharkawi LY. Search for hidden chambers in the pyramids. 1970.

[23] Tanaka HK, Taira H, Uchida T, Tanaka M, Takeo M, Ohminato T, *et al.* Three‐dimensional computational axial tomography scan of a volcano with cosmic ray muon radiography. *Journal of Geophysical Research: Solid Earth* 2010;**115**.

[24] Tanaka H, Nakano T, Takahashi S, Yoshida J, Takeo M, Oikawa J, *et al.* High resolution imaging in the inhomogeneous crust with cosmic-ray muon radiography: The density structure below the volcanic crater floor of Mt. Asama, Japan. *Earth and Planetary Science Letters* 2007;**263**:104-113.

[25] Ambrosi G, Ambrosino F, Battiston R, Bross A, Callier S, Cassese F, *et al.* The MU-RAY project: Volcano radiography with cosmic-ray muons. *Nuclear Instruments and Methods in Physics Research Section A: Accelerators, Spectrometers, Detectors and Associated Equipment* 2011;**628**:120-123.

[26] Tanaka HKM, Taira H, Uchida T, Tanaka M, Takeo M, Ohminato T, *et al.* Three-dimensional computational axial tomography scan of a volcano with cosmic ray muon radiography. *Journal of Geophysical Research* 2010;**115**.

[27] Gnanvo K, Grasso LV, Hohlmann M, Locke JB, Quintero A, and Mitra D. Imaging of high-Z material for nuclear contraband detection with a minimal prototype of a muon tomography station based on GEM detectors. *Nuclear Instruments and Methods in Physics Research Section A: Accelerators, Spectrometers, Detectors and Associated Equipment* 2011;**652**:16-20.

[28] Tanaka HKM. Particle Geophysics. *Annual Review of Earth and Planetary Sciences* 2014;**42**:535-549.

[29] Gaisser TK, *Cosmic rays and particle physics*: Cambridge University Press, 1990.

[30] Sternheimer RM. The density effect for the ionization loss in various materials. *Physical Review* 1952;**88**:851.

[31] Groom DE, Mokhov NV, and Striganov SI. Muon stopping power and range tables 10 MeV–100 TeV. *Atomic Data and Nuclear Data Tables* 2001;**78**:183-356.

[32] Mei DM, Zhang C, Thomas K, and Gray F. Early results on radioactive background characterization for Sanford Laboratory and DUSEL experiments. *Astroparticle Physics* 2010;**34**:33-39.

[33] Birkholzer, J., Q. Zhou & C. Tsang. Large-scale impact of CO_2 storage in deep saline aquifers: A sensitivity study on pressure response in stratified systems. *International Journal of Greenhouse Gas Control* 2009;**3**:181-194.

[34] Agostinelli S, Allison J, Amako KA, Apostolakis J, Araujo H, Arce P, *et al.* GEANT4—a simulation toolkit. *Nuclear instruments and methods in physics research section A: Accelerators, Spectrometers, Detectors and Associated Equipment* 2003;**506**:250-303.

[35] Arslan H and Bektasoglu M. Geant4 Simulation Study of Deep Underground Muons: Vertical Intensity and Angular Distribution. *Advances in High Energy Physics* 2013;**2013**.